Ultraviolet Absorption of Insulators. IV. Rare-Gas Solids*

J. C. PHILLIPS†
Department of Physics and Institute for the Study of Metals, University of Chicago, Chicago, Illinois

(Received 12 March 1964, revised manuscript received 1 June 1964)

The analysis of the fcc alkali halides given in III is extended to the rare-gas solids, especially Xe. The interband spectrum is similar to the alkali halides. The valence bands of Xe are narrow compared to the spin-orbit splitting, which produces extra structure in the one-electron spectrum. The orbital valence band width at L is 0.5 eV, in agreement with band calculations. The lower lying conduction bands are nearly free electron in character. Because the crystal is monatomic with only neutral lattice defects, the coherent exciton spectrum is well resolved. Again, an intimate connection is established between the interband edges and both hydrogenic and extra excitons (those not associated with the edge at Γ). Exciton-exciton configuration interactions mediated coherently by the photon field and incoherently (dissipatively) by the phonon field are studied qualitatively. According to the general scattering theories of Fano and Van Hove, certain relations are expected to hold between diagonal and off-diagonal elements of the exciton-photon and exciton-phonon self-energies. It is demonstrated qualitatively that these relations hold, and that they account not only for asymmetries of individual resonance lines but also for the entire pattern of resonances and antiresonances in Xe. In particular, previously unexplained anomalies in the Rydberg spectra of the "halogen doublets" are shown to be direct consequences of exciton-exciton configuration interaction mediated by the coherent photon field.

1. INTRODUCTION

IN the preceding paper[1] we have analyzed the ultraviolet absorption spectra of fcc alkali halides. We have shown how the spectral structure can be divided into exciton and scattering parts, and interpreted each part in detail. A somewhat disappointing feature of the alkali halide spectra is the comparative paucity of fine structure in many crystals. For example, in most cases only the $1s$ exciton state is resolved for each class of exciton. For shallow excitons in semiconductors, a Rydberg series of $1s$, $2s$, $\cdots$ excitons is often resolved.

The fcc alkali halides may be regarded as a complex version of the rare-gas solids, which also condense in a fcc lattice. Alkali halide crystals (especially evaporated films) generally contain charged defects which couple electrons, holes, and excitons strongly to the lattice. In well annealed rare-gas-solid films, the coupling to the lattice can be made quite weak. The degree of coupling can be controlled through the degree of annealing of the evaporated film. A series of experiments might be possible in which the particle-lattice coupling is varied in an almost ideal manner.

Baldini has recently carried out elegant measurements[2] of the ultraviolet absorption spectra of solid Ar, Kr, and Xe. The experimental technique, based on differential phosphor luminescence, minimizes surface effects and produces spectra apparently comparable, or superior even, to those of Eby, Teegarden, and Dutton for the alkali halides.[3] The spectrum of annealed Xe shows Rydberg series both for the $\Gamma(\frac{3}{2})$ exciton and the $\Gamma(\frac{1}{2})$ exciton. The $1s$ Γ excitons have been discussed by Baldini, who has shown that their excitation energy agrees within a few hundredths of an electron volt with the respective atomic triplet and singlet resonance lines.

Our purpose here is threefold. First, we continue the analysis of Baldini's spectra to higher energies (Sec. 2). Second, we examine the role of exciton-photon self-energies in determining the positions of exciton resonances and antiresonances (Sec. 3). Third, we discuss the role of exciton-lattice self-energies in damping the resonances and altering the line shape of interband thresholds (Sec. 4). The theoretical significance of our results is summarized in Sec. 5, where suggestions for further experiments are made.

2. SCATTERING AND EXCITON SPECTRA

We begin our analysis with the annealed Xe spectrum shown in Fig. 1. The spin-orbit splitting $3\lambda/2$ of the $\Gamma(\frac{3}{2})-\Gamma(\frac{1}{2})$ excitons at 8.36 and 9.53 eV is 1.17 eV. As pointed out by Baldini, the $\Gamma(\frac{3}{2})$ exciton exhibits a Rydberg series of $2s$ and $3s$ states at 9.07 and 9.19 eV, respectively. The calculated series limit is 9.28 eV, which is the position of the fourth peak.

One can also recognize the $2s$ $\Gamma(\frac{1}{2})$ exciton at 9.75 eV, and the series limit at 9.90 eV. The binding energy of the $1s$ $\Gamma(\frac{1}{2})$ exciton (0.33 eV) is enormously reduced compared to the $1s$ $\Gamma(\frac{3}{2})$ exciton (0.92 eV). We will demonstrate in Sec. 4 that this reduction is a consequence of exciton-exciton interaction mediated coherently by the photon field.

The L excitons in Xe fall at 10.30 and 11.15 eV. The splitting of 0.85 eV is greater than $\lambda=0.79$ eV. In the

* This work has been supported in part directly by the U. S. Office of Naval Research and the National Science Foundation. In addition, it has benefited indirectly through partial support of solid state theory by the National Aeronautics and Space Administration, of the Low Temperature Laboratory of the Institute for the Study of Metals by the National Science Foundation, and of Materials Sciences at the University of Chicago by the Advanced Research Projects Administration.

† Alfred P. Sloan Fellow.

[1] J. C. Phillips (preceding paper), Phys. Rev. **136**, A1705 (1964).

[2] G. Baldini, Phys. Rev. **128**, 1562 (1962).

[3] J. E. Eby, K. J. Teegarden, and D. B. Dutton, Phys. Rev. **116**, 1099 (1959).

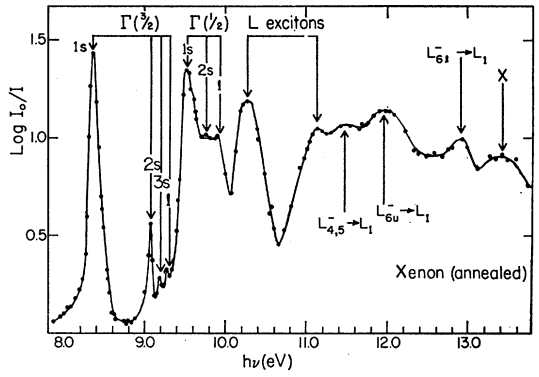

FIG. 1. The absorption spectrum of solid Xe (annealed at 53°K) at 21°K.

alkali halides, the splitting of the L exciton was about $2\lambda/3$, that is, about $\frac{2}{3}$ the splitting of $L_{3'}$. The enhanced spin-orbit splitting of the L excitons will be understood by considering the interband scattering spectra.

The band structure of solid Ar has been calculated by Knox and Bassani,[4] and by Mattheiss.[5] Their results are shown in Figs. 2 and 3 (the effects of spin-orbit splitting have been omitted).

It is evident that although the valence bands are rather similar, there are great differences in the conduction band levels. Mattheiss points out[5] that this is due to the omission by Knox and Bassani of d levels, which are difficult to treat by their orthogonalized-plane-wave (OPW) method.[6,7] The transitions $3p^6 \rightarrow 3p^5 3d$ are prominent in the spectrum of free Ar also. We therefore sketch in Fig. 4 our bands for Xe by following the results of Fig. 3.

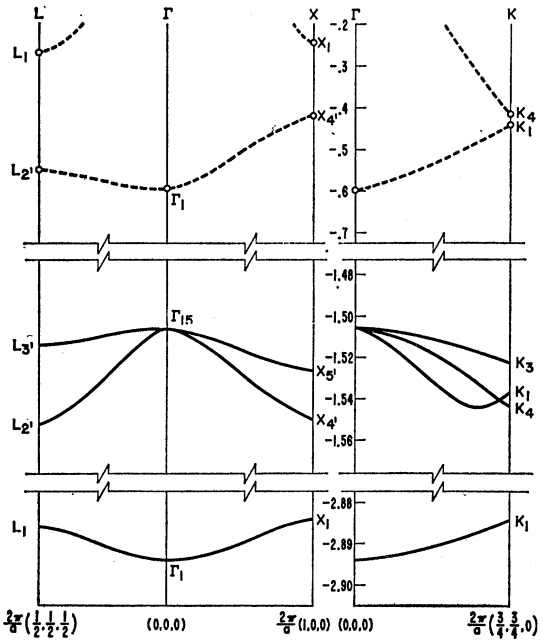

FIG. 2. The energy bands of Ar according to Knox and Bassani (Ref. 4).

An interesting feature of Mattheiss' calculations is that the center of gravity of L_1 and $L_{2'}$ is 3.5 eV above Γ_1, in agreement with the nearly free electron model. It follows that the success of this model for these two levels does not determine the position of the d bands $\Gamma_{25'}$ and Γ_{12} very strictly. [However, $\Gamma_{25'}$ must be at least 1 or 2 eV above $E_f(L)$.]

The valence bandwidth between Γ_{15}, $L_{3'}$, and $X_{5'}$ was 1 to 2 eV for the alkali halides. The same width in Ar is about 0.2 eV. Indeed, the valence states $L_{2'}$ and $X_{4'}$, which played no role in the alkali halide discussion, are only about 0.5 eV below Γ_{15}. In Xe, where the spin-orbit splitting is 1.2 eV, these states are quasidegenerate with $L_{3'}$ and $X_{5'}$ respectively, with regard to the spin-orbit interaction.

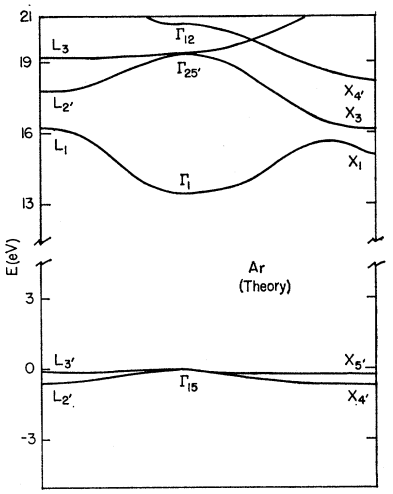

FIG. 3. The energy bands of Ar as obtained by Mattheiss using the augmented-plane-wave method.

We treat this problem using Elliott's sketch[8] of the energy bands of the fcc or diamond lattices including spin-orbit coupling effects. The set of quasidegenerate orbital levels ($L_{3'}$; $L_{2'}$) become the double group representations ($L_4^- + L_5^-$, L_6^-; L_6^-). From Kane's curves[9] for $E(k)$ along $\langle 111 \rangle$ axes, one can derive the splitting of these quasidegenerate levels in terms of λ and the orbital splitting

$$W_L = L_{3'} - L_{2'} \tag{2.1}$$

in the absence of spin-orbit coupling. Let the upper and lower L_6^- levels be L_{6u}^- and L_{6l}^-, respectively. One

[4] R. S. Knox and F. Bassani, Phys. Rev. **124**, 652 (1961).
[5] L. F. Mattheiss, Phys. Rev. **133**, A1399 (1964).
[6] Somewhat more complete convergence for d-like states such as Γ_{12} has been obtained using OPW's by Fowler.
[7] W. B. Fowler, Phys. Rev. **132**, 1591 (1963).
[8] R. J. Elliott, Phys. Rev. **96**, 130 (1954).
[9] E. O. Kane, Phys. Chem. Solids **1**, 83 (1956).

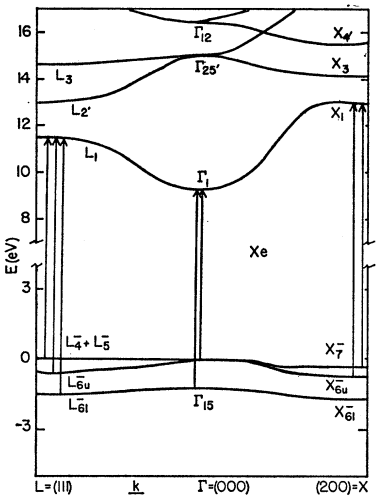

FIG. 4. The energy bands of Xe as inferred from experiment by analogy with Fig. 3. The double-group notation is used for the valence band, the single-group for the conduction band.

finds to a good approximation ($W_L \ll 3\lambda/2$)

$$(L_4^- + L_5^-) - L_{6u}^- = W_L \tag{2.2}$$

$$\tfrac{1}{2}B_L + L_{6u}^- - L_{6l}^- = 3\lambda/2. \tag{2.3}$$

The calculated value of W_L in Ar is about 0.5 eV. With $3\lambda/2 = 1.2$ eV, we see that the interband peaks at 11.5, 12.0, and 12.9 eV can be assigned to the M_1 Van Hove edges

$$(L_4^- + L_5^-) \rightarrow L_1 \quad 11.5 \text{ eV},$$
$$L_{6u}^- \rightarrow L_1 \quad 12.0 \text{ eV},$$
$$L_{6l}^- \rightarrow L_1 \quad 12.9 \text{ eV}.$$

This completes our analysis of the Xe interband spectrum. If one compares the spectrum of Xe with that of KBr, KI, and RbI, it is tempting to assign the peak Y in the alkali halides (see, e.g., Fig. 1 of III) to transitions starting from the valence state $L_{2'}$. The flaw in this assignment is that Y is strongest in KBr, where we have positive evidence that $L_{2'}$ is the lowest conduction band state. Dipole transitions $L_{2'} \rightarrow L_{2'}$ are of course forbidden by parity.

We are now in a position to understand the unusual L exciton spectrum. The peak at 10.30 eV is abnormally broad because its parent interband edges are the quasi-degenerate $(L_4^- + L_5^-,\ L_{6u}^-) \rightarrow L_1$. The spin-orbit splitting is unusually large because it includes the bandwidth due to $L_{3'} - L_{2'}$.

We can use Mattheiss' band structure for Ar (Fig. 3) to construct a semiempirical band structure for Xe (Fig. 4). (We use the single-group notation for the conduction band, and the double-group notation to describe the spin-orbit splittings of the valence band at L and X.)

We have identified the structure near 13.3 and 13.8 eV with $(X_7^-,\ X_{6u}^-) \rightarrow X_1$. If the d levels $\Gamma_{25'}$ and Γ_{12} were lower in energy, the final state for their structure could be X_3. (Transitions to X_1 might be buried under the L transitions, although this seems unlikely.) Further experimental data between 13 and 15 eV would be helpful here.

There is so little structure presently known in the Ar spectrum that we will not discuss it. In the Kr spectrum, the $1s\Gamma(\frac{3}{2})$ and $1s\Gamma(\frac{1}{2})$ excitons are at 10.17 and 10.81 eV, with $3\lambda/2 = 0.64$ eV. It is possible that the L excitons are at 11.25 and 11.94 eV, but this gives too large a spin-orbit splitting. We therefore concur with Baldini that the peaks (10.17, 11.24, 11.48) constitute the $\Gamma(\frac{3}{2})$ ($1s$, $2s$, $3s$) Rydberg series, with the series limit at 11.65 eV $= \Gamma_1 - \Gamma_{15}^{3/2}$. It also appears that the exciton peak at 11.95 eV is the $2s\Gamma(\frac{1}{2})$ exciton, as suggested by Baldini. In that case, we note that the binding energy of $1s\Gamma(\frac{1}{2})$ excitons is only 1.52 eV compared to 1.73 eV for the $\Gamma(\frac{3}{2})$ excitons.

3. EXCITON-PHOTON INTERACTIONS

The exciton-photon field in the crystal is coherent in the following sense. If we neglect all interband transitions except those which conserve crystal momentum k, then the $l=0$ partial wave exciton resonances constitute additional normal modes for the electromagnetic field in the crystal, when only allowed interband transitions are considered. (First-order forbidden interband edges give rise to weak $l=1$ exciton resonances which we usually neglect.[10]) Also, electron-hole pairs in unbound scattering states must be regarded as the normal (nonresonant) modes for photons propagating in the crystal. Above the interband threshold of the perfect crystal, this situation is not unexpected. The resonant states interfere with the scattering states in a way well known from the Breit-Wigner theory of nuclear resonances.[11,12] The interference leads to asymmetric resonances if no incoherent (dissipative) channels are present.[12] A good example of an isolated asymmetric resonance above the direct threshold is found[13] at 3.5 eV in CdTe.

Below the interband threshold, there is always some background absorption associated with volume defects or surface effects. Making the "optical-model" or "configuration-average" approximation,[14] we assume that the background absorption is a volume effect distributed uniformly throughout the crystal. Then we also expect interference between an isolated exciton resonance and the background itself, leading to an asymmetric line followed by an antiresonance. Such interference has been observed by several workers.[15] We emphasize that it occurs in general for isolated reso-

[10] R. J. Elliott, Phys. Rev. **108**, 1384 (1957).
[11] M. A. Preston, *Physics of the Nucleus* (Addison-Wesley Publishing Corporation, Reading, Massachusetts, 1962), p. 503.
[12] U. Fano, Phys. Rev. **124**, 1868 (1961).
[13] J. C. Phillips, Phys. Rev. Letters **12**, 447 (1964).
[14] Y. Toyozawa, Progr. Theoret. Physics (Kyoto) **20**, 53 (1958).
[15] F. Fischer, Z. Physik **139**, 238 (1954); W. Martienssen, Phys. Chem. Solids **2**, 256 (1957); L. P. Zuerev, M. M. Noskov, and M. Ya. Shur, Fiz. Tverd. Tela **2**, 2643 (1960) [English transl.: Soviet Phys.—Solid State **2**, 2357 (1961)]; S. Nikitine (unpublished).

nances. It is not solely an exciton-exciton interference effect mediated by the phonon field, as suggested by several workers.[16–18] We return to this point, which is central to the theory of coherent and incoherent scattering, in the next section.

We turn now to exciton-exciton configuration interactions mediated by photons. In our case, we have two major classes C of excitons, hydrogenic, $C=H$, or metastable, $C=M$. The hydrogenic excitons are labeled by the parent hole states $J=\frac{3}{2}$ or $J=\frac{1}{2}$. The metastable excitons can also be labeled by $J=\frac{3}{2}$ or $J=\frac{1}{2}$, providing that we remember that there is an orbital splitting of the $\frac{3}{2}$ valence states at L into $(L_4^-+L_5^-)$ and L_{6u}^- (see Fig. 4). The hydrogenic excitons exhibit a Rydberg series $n=1, 2, \cdots$, etc. Thus the exciton resonances are labeled by $\alpha=(C,J,n)$ in our case. The possibility of higher exciton resonances above 14 eV is neglected.

Neglecting the coherence of the exciton-(scattering electron-hole)-photon field, we would expect the imaginary part of the dielectric constant to be given additively by

$$\epsilon_2(\omega,g)=\epsilon_2(\omega,0)+C\sum_\alpha \frac{\Gamma_\alpha}{(\hbar\omega-\epsilon_\alpha)^2+\Gamma_\alpha^2}. \quad (3.1)$$

Here g is the actual value of the electron-hole coupling constant, and $\epsilon_2(\omega,0)$ is the scattering interband term, providing we neglect subtraction of oscillator strength from the one-electron interband spectrum by the exciton resonances.

Because of coherence, we cannot add intensities as in (3.1). According to Fano,[12] we must treat the exciton-photon field by an equivalent Hamiltonian which represents the real part of exciton-photon self-energies. Starting from the unperturbed (noninteracting) resonances, the equivalent Hamiltonian has the form,

$$\mathcal{H}_{\alpha\alpha'}{}^e=\epsilon_\alpha\delta_{\alpha\alpha'}+\delta\epsilon_{\alpha\alpha'}(1-\delta_{\alpha\alpha'}). \quad (3.2)$$

Diagonalizing (3.2), we obtain the actual resonant energies E_β. We now introduce the binding energies B_α of the noninteracting exciton resonances which are defined as the difference in energy between ϵ_α and the parent interband-scattering edge at ξ_α. For hydrogenic excitons,

$$\xi_\alpha-\epsilon_\alpha=B_\alpha=g^2b_\alpha, \quad (3.3)$$

where b_α is independent of g.

Fano gives a general expression for $\delta\epsilon_{\alpha\alpha'}$ which is

$$\delta\epsilon_{\alpha\alpha'}(E)=g^2P\int dE'\frac{V_{\alpha E'}V_{E'\alpha'}}{E-E'}. \quad (3.4)$$

Here $V_{\alpha E'}$ is the scattering amplitude caused by the (screened) Coulomb interaction gV from resonant state α to scattering state labeled by E'.

It is intended that (3.4) describe the diagonal exciton-photon self-energies $\delta\epsilon_{\alpha\alpha}$. However, as the notation of (3.2) and (3.4) is meant to suggest, it is clear that the difference between ϵ_α and the energy of the interband scattering edge ξ_α, i.e., B_α, is just $\delta\epsilon_{\alpha\alpha}$ (calculated in Born approximation). We have therefore absorbed $\delta\epsilon_{\alpha\alpha}$ into ϵ_α.

To estimate the order of magnitude of $\delta\epsilon_{\alpha\alpha'}$, we replace the energy denominator in (3.4) by a mean energy (α-independent) and obtain the qualitative result,

$$(\delta\epsilon_{\alpha\alpha'})^2\lesssim B_\alpha B_{\alpha'}. \quad (3.5)$$

We have introduced (3.5) not for quantitative purposes, but merely to illustrate the notion that for a family of exciton resonances, the real parts of off-diagonal exciton-photon self-energies are comparable to diagonal parts.

Having introduced the eigenvalues E_β, we introduce also the Breit-Wigner decay widths Γ_β; and following Fano, we define the phase shift Δ_β associated with a given resonance by

$$\tan\Delta_\beta(E)=\Gamma_\beta/(E-E_\beta). \quad (3.6)$$

Because the field is coherent, Fano introduces the collective phase shift Δ given by

$$\tan\Delta(E)=\textstyle\sum_\beta \tan\Delta_\beta(E). \quad (3.7)$$

Let the oscillator amplitude for a given resonance be q_β. Then the correct generalization of (3.1) (within the random-phase approximation[19]) to include coherence effects is

$$\epsilon_2(\omega,g)=\cos^2\Delta(\textstyle\sum_\beta q_\beta\tan\Delta_\beta-1)^2\epsilon_2(\omega,0). \quad (3.8)$$

From (3.8) we obtain a series of alternating resonances and antiresonances. When only one resonance is present in (3.8), we still obtain an asymmetric resonance as well as an antiresonance because of interference with the scattering background. When one measures absorption coefficients, the antiresonance between two resonances of approximately equal strength with a nearly constant background takes the form of a symmetrical V. Two such V's are seen in Fig. 1 at 10.05 and 10.65 eV.

We are now in a position to discuss the remarkable fact noted in Sec. 2: for Xe, $E(H,\frac{3}{2},\infty)-E(H,\frac{3}{2},1)=0.92$ eV, while $E(H,\frac{1}{2},\infty)-E(H,\frac{1}{2},1)=0.37$ eV. Now the only difference between the $J=\frac{3}{2}$ and $J=\frac{1}{2}$ excitons lies in the contribution of the hole to the reduced mass

$$\mu^{-1}(J)=m_e{}^{-1}+m_h{}^{-1}(J). \quad (3.9)$$

However, as pointed out by both Baldini[2] and Fowler,[7] $m_e\lesssim 0.5m$, while $m_h(J)\gtrsim 4m$ for both $J=\frac{3}{2}$ and $\frac{1}{2}$. The

[16] R. J. Elliott, *Proceedings of the Conference on Semiconductor Physics* (Czechoslovakian Academy of Science, Prague, 1961), p. 408; J. J. Hopfield, Phys. Chem. Solids **22**, 63 (1961).

[17] Hopfield (Ref. 16) has also stressed that the asymmetry obtains whenever a resonance amplitude is superposed on a continuum amplitude, *regardless* of the origin of the continuum. Our viewpoint agrees with his.

[18] Y. Toyozawa, Phys. Chem. Solids **25**, 59 (1964).

[19] H. Ehrenreich and M. H. Cohen, Phys. Rev. **115**, 786 (1959).

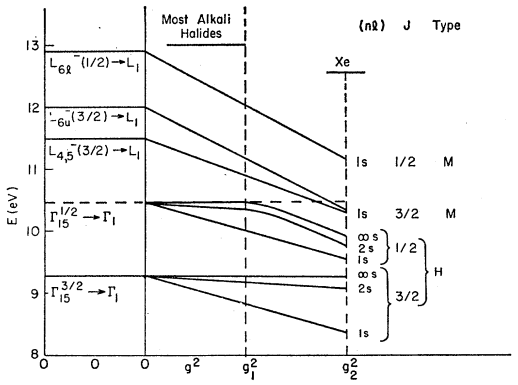

FIG. 5. A plot of the coherent exciton spectrum for $l=0$ as a function of the electron-hole coupling constant g. When $g=0$, we have only the one-electron interband scattering spectrum shown at the left. As g is increased, collective resonances corresponding to bound electron-hole pairs are detached both from interband thresholds (Van Hove edges M_0) and from interband saddle points (Van Hove edges M_1). The former are called hydrogenic excitons, the latter metastable excitons. Because of the coherent character of the exciton field, as g is increased no level crossings occur. This causes a distortion of the weak $H(J=\frac{1}{2})$ excitons for $n\geq 2$ and $g\gtrsim g_1$, which appears as a bending of their energies. The energy scale used applies explicitly to Xe. The results for alkali halides are qualitatively similar so far as the one-electron band edges are concerned. Because dielectric screening is stronger in the alkali halides, g^2 ranges from $\frac{1}{4}$ to $\frac{1}{2}$ the value in Xe, and only small interactions between hydrogenic and metastable excitons ordinarily occur.

Rydberg series holds rather well for the $J=\frac{3}{2}$ excitons, which means that using (3.9) one cannot explain the apparent difference in binding energy for the hydrogenic excitons $J=\frac{3}{2}$ and $J=\frac{1}{2}$. On the other hand, using Fano's approach, we see that the strong $J=\frac{3}{2}$ metastable exciton resonance at L has shifted the weak $J=\frac{1}{2}$ ($2s$ and lim) hydrogenic exciton resonances by $\epsilon_\alpha - E_\alpha \sim 0.5$ eV.

We plot in Fig. 5 the important exciton levels as a function of g^2. Using this plot and applying the general Breit-Wigner theory[11,12] to exciton-continuum interference and exciton-exciton-interference, one can infer almost by inspection the effect of exciton-exciton interaction on the position and line shape of collective resonances and antiresonances. For $g=0$ we have the observed interband edges on the left of the figure. For small $g\sim g_1$,

$$B(M,\tfrac{3}{2},1)\ll(L_{45}^{-}\to L_1)-(\Gamma_{15}^{1/2}\to\Gamma_1), \quad (3.10)$$

and in this limit the interaction between metastable excitons and hydrogenic excitons can be neglected. (This limit apparently corresponds to most alkali halides.) The difference between the series limit and the $1s$ state is the same for both $J=\frac{1}{2}$ and $J=\frac{3}{2}$ hydrogenic families. The series limits coincide with the respective interband edges.

In the strong coupling limit $g\sim g_2$, a number of interesting effects occur. The most striking is the depression of the hydrogenic $J=\frac{1}{2}(ns)$ levels for $n\geq 2$. Because of this depression, the $J=\frac{1}{2}$ limit resonance no longer coincides with the interband threshold, which is buried at 10.45 eV beneath the lower metastable exciton. We also see that the latter is composite, which accounts for its broad, symmetrical resonance character. Experiments on very well annealed films at He temperatures might resolve the composite structure.

To our knowledge, the exciton spectra discussed above represent the first clear-cut case of strongly interacting collective excitations which can be observed in both the weak-coupling ($g=0$) limit and the strong coupling limit. In superconductors, the binding energy of Cooper pairs can be varied from 0 at $T=T_c$ to a maximum at $T=0$, but attempts to demonstrate a second set of collective states (d pairing) have so far proved inconclusive. In particular, incoherent quenching of the collective states (observed here) is expected[20] in superconductors but is not observed.[20]

It may be possible to study two-photon absorption into $l=1$ exciton resonances. While the np Rydberg series is trivial, it is amusing to consider Reggeizing[21] the p states of metastable excitons. It would also be amusing to study the effects of uniaxial strain using polarized photons: This is an elementary example of broken symmetry.[22]

We conclude this section by discussing the exciton spectrum[23] of substitutional Xe impurities in Ar. It is not surprising that the spectrum shows two hydrogenic series. What is extremely remarkable is that metastable excitons $(L,\frac{3}{2})$ exist at 11.0 eV with a line shape not very different from that in the pure Xe crystal. This implies that the presence of the Xe atom modifies the continuum in its vicinity in such a way that Van Hove interband edges are still present, and are not broadened (because k is no longer a good quantum number) by more than 2 eV (the binding energy of the L excitons). Again these exciton resonances interact with the hydrogenic $J=\frac{1}{2}$, $n\geq 2$ excitons. Again the difference between the series limit and the $1s$ ground state is 2.23 eV for the $J=\frac{3}{2}$ series, and only 0.3 eV for the $J=\frac{1}{2}$ series. Here, localization near the impurity enforces noncrossing of exciton levels belonging to different families.

In Rn, the spin-orbit splitting of the valence band should be about 3.5 eV. This would lead to a reversal of the positions of $E_H^{1/2}(1s)$ and $E_M^{3/2}(1s)$, which would be equivalent to a larger value of g^2 in Fig. 5. We realize the difficulty of securing sufficient pure Rn, but it would be of great theoretical interest to know the form of the $E_H^{1/2}(ns)$ spectrum when it falls in the antiresonance region between the $J=\frac{1}{2}$ and $J=\frac{3}{2}$ metastable excitons.

[20] K. Maki and T. Tsuneto, Progr. Theoret. Phys. (Kyoto) **28**, 163 (1962); J. D. Leslie and D. M. Ginsberg, Phys. Rev. **133**, A362 (1964).
[21] E.g., M. Gell-Mann, M. Goldberger, F. Loew, V. Singh, and F. Zachariasen, Phys. Rev. **133**, B161 (1964).
[22] M. Gell-Mann, Phys. Rev. **125**, 1067 (1962).
[23] G. Baldini and R. S. Knox, Phys. Rev. Letters **11**, 227 (1963).

4. EXCITON-PHONON SELF ENERGIES

The effect of exciton interactions with lattice vibrations and lattice defects has been treated for excitons below the interband threshold by several workers, especially Toyozawa.[14,18] Neglecting spatial dispersion, exciton-defect scattering and exciton-phonon scattering are qualitatively similar in Born approximation. Henceforth we include exciton-defect scattering in exciton-phonon scattering by appropriate adjustment of the phonon temperature,[14] which is qualitatively similar to adjusting the exciton-phonon coupling strength g'.

The central difference between coherent and incoherent self-energies of spatially extended wave packets has been stressed by Van Hove.[24] He notes that the second- and higher order contributions of coherent interaction to off-diagonal self-energies is generally comparable to the diagonal contribution [e.g., Eq. (3.5)]. On the other hand, for incoherent interactions, if the wave packet extends over N atomic cells, higher order off-diagonal self-energies are smaller than diagonal self-energies by a factor of order N. For shallow excitons, the smallness of off-diagonal (interband) self-energies compared to diagonal (intraband) energies has been demonstrated explicitly by Toyozawa.[14] However, in order to explain the observed asymmetries,[15] he and other workers[16,17] have appealed to incoherent off-diagonal phonon self-energies, although quantitative estimates[18] show that even in the weak coupling limit the energies are too small by a factor of 2 or 3. In Xe we are dealing with incoherent self-energies $\gamma_{\alpha\alpha'}=\gamma_{\alpha\alpha'}'+i\gamma_{\alpha\alpha'}''$, whose diagonal components are of order 0.1–0.2 eV with $\hbar\omega_D \lesssim 0.005$ eV. Thus we are in the strong coupling limit, and the off-diagonal components $\gamma_{\alpha\alpha'}$, $\alpha' \neq \alpha$, may be neglected. The line shape of the exciton resonances can be obtained directly by folding (3.8) with a Gaussian broadening factor $\gamma(E)$, which is equal to $\gamma_{\alpha\alpha}(E_\alpha)$ when $E=E_\alpha$, and varies smoothly as a function of E.

In general, the resonant energies E_α are found to shift as the exciton-lattice coupling strength g' is increased, either through raising the temperature or increasing the number of lattice defects. For large g', this shift in $\gamma_{\alpha\alpha}'$ can be calculated from second-order perturbation theory.[14] Let us suppose that the range of intermediate states i which contribute to

$$\gamma_{\alpha\alpha}' \sim g'^2 \sum_{\omega_D} \left[\frac{P(1+n(\omega_D))}{E_\alpha - E_i - \hbar\omega_D} + \frac{Pn(\omega_D)}{E_\alpha - E_i + \hbar\omega_D} \right] \quad (4.1)$$

is large,

$$B_\alpha / \langle E_i - E_\alpha \rangle = \eta \lesssim 1. \quad (4.2)$$

Then it is easy to show that to lowest order in η, the shift in energy $\delta\xi_\alpha$ of the parent interband edge is the same as the change in exciton-lattice self-energy $\delta\gamma_\alpha'$. Thus B_α is almost constant (first order in η).

[24] L. Van Hove, Physica **21**, 517, 901 (1955).

TABLE I. The dependence of exciton self-energies on the strength of lattice coupling. The threshold for direct transitions is E_g, while $1s$ excitons are centered at $\epsilon(1s)$. When the lattice coupling is increased, the threshold and exciton energy shift by δE_g and $\delta\epsilon(1s)$, respectively.

	E_g		$\epsilon(1s)$		δE_g	$\delta\epsilon(1s)$
T(°K)	80	300	80	300		
RbI	6.05	5.83	5.72	5.54	−0.22	−0.18
KBr	7.76	7.60	6.77	6.58	−0.19	−0.14
KI	6.08	5.92	5.80	5.62	−0.16	−0.18
Defects	Few	Many	Few	Many		
Xe	9.28	9.28	8.36	8.53	0.00	+0.17

This point is illustrated for large g' in Table I for the alkali halide crystals.[3] Both E_g and $\epsilon(1s)$ decrease between nitrogen temperature and room temperature, as required by second-order perturbation theory, and by the same amount (to within 10%). The results[2] for Xe (small g') shown in the last line of the table contradict second-order perturbation theory not only quantitatively—there is no shift in E_g but a large shift in $\epsilon(1s)$—but also qualitatively, because the defect-induced coupling *increases* $\epsilon(1s)$, i.e., quenches part of the exciton binding energy $B(H,\frac{3}{2},1)$, as shown in Fig. 6.

The resolution of this puzzle appears to lie in generalization of Toyozawa's isotropic model to include anisotropic effects. The most important of these is the anisotropy of the wave-number dependent dielectric function[25] $\epsilon(q)$. One can then see that the binding energy will contain an anisotropic component which can be quenched by lattice scattering. The quenching is first-order in the exciton-lattice coupling g'. The situation is similar to the quenching of gap anisotropy in dirty superconductors.[26,27]

When the lifetime broadening is so great as to wash out the ns excitons for $n \geq 2$, as in unannealed Xe, one may ask where the oscillator strength associated with these bound states is now found. Some of it may be transferred to the $1s$ excitons, some to the direct scatter-

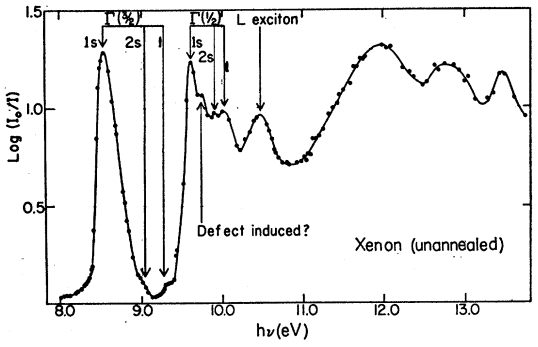

FIG. 6. The absorption spectrum of unannealed solid Xe at 19°K.

[25] W. Cochran and J. C. Phillips, Phys. Rev. **135**, A1402 (1964).
[26] P. W. Anderson, Phys. Chem. Solids **11**, 26 (1959).
[27] P. L. Richards, Phys. Rev. Letters **7**, 412 (1961).

ing threshold. Again there is an analogy to the quenching of collective exciton states in superconductors.[20]

It appears that in annealed Xe, for the $\Gamma(\frac{3}{2})$ excitons the weak peak at 11.65 eV is the Elliott shoulder[10] which includes some of the oscillator strength of ns excitons ($n \geq 4$). In the unannealed films, the $3s$ exciton as well as part of the $2s$ exciton must also be absorbed into the Elliott shoulder. (Part of the $2s$ exciton remains as the high energy foot of the broadened $1s$ exciton.) The oscillator strength of ns excitons varies as n^{-3} in the hydrogenic model, which fits the annealed $1s$, $2s$, and $3s$ peaks in Xe quite well. Thus, adding the $3s$ exciton and part of the $2s$ exciton to the Elliott shoulder increases its oscillator strength by about a factor of 5.

It is apparent that the discussion for unannealed Xe can be carried over to the alkali halides. There the short lifetimes due to longitudinal optical phonon emission completely quench the $n \geq 2$ excitons, and give an Elliott shoulder stronger than in unannealed Xe.

It is of interest to examine the shift in the real part $\gamma'(M,\frac{3}{2})$ of the self-energy of the $m_J=\frac{3}{2}$ metastable L exciton caused by defects. The $L_{4,5}^- \rightarrow L_1$ interband edge is difficult to resolve in the unannealed spectrum, partly because of the broadening of the $m_J=\frac{1}{2}$ metastable exciton. The $L_6^- \rightarrow L_1$ interband edge is shifted at most from 12.00 to 11.95 eV. This agrees with the absence of a shift in the interband threshold $\Gamma_{15}(\frac{3}{2}) \rightarrow \Gamma_1$. The change in $\gamma'(M,\frac{3}{2})$ is $+0.18 \pm 0.03$ eV, which is essentially the same as the change of $+0.17$ eV quoted for the $\Gamma(\frac{3}{2})$ exciton. Thus the anisotropic contribution to $B(M)$ is probably much the same as the anisotropic contribution to $B(H)$.

5. CONCLUSIONS

It is apparent from the discussion we have given that the optical spectrum of Xe is extraordinarily rich in many-body effects. The present paper discusses a few of these effects qualitatively. A more complete theoretical analysis of the line shape based on the Breit-Wigner-Fano theory is being made by Jain.[28] It appears that Xe may well play the role among insulators that the alkalies play among metals, and Si and Ge play for semiconductors.

Up to 11 eV, the spectrum is dominated by exciton interference effects. We have demonstrated exciton-exciton configuration interactions mediated by the photon field in Sec. 3. In Sec. 4 we suggested that exciton-exciton interactions mediated by the lattice are negligible. For an isolated exciton resonance, we suggested that dissipative phonon interactions may interfere with exciton-photon interactions and quench anisotropic contributions to the exciton-photon self-energy.

Because the antiresonances in the annealed Xe film are quite sharp, it would be interesting to know whether the (incoherent) absorption at the bottom of an antiresonant V is primarily caused by surface scattering, vacancies, or spontaneous phonon emission. The antiresonances provide the best test for the quality of the film, and it would be interesting to study the magnitude of antiresonances in well annealed films from low temperatures up to the melting point. Correlation of the magnitude of the antiresonance with the broadening of, e.g., the $(M,\frac{1}{2})$ resonance near 11 eV, might lead to a better understanding of the way resonances "dissolve" into background[29] (as this resonance does in the unannealed film).

Further experiments on resonance families should attempt to obtain ϵ_2 either directly by polarimetry or through Kramers-Kronig transforms. Theoretical expressions like (3.8) can be Kramers-Kronig transformed if one makes certain assumptions about the high-energy values of ϵ_2, but in practice it seems preferable to carry out dispersion transforms of the original data.

Note added in proof. The central new idea which we have advanced concerns the generation of extra exciton resonances (which we have called metastable excitons) associated with saddle-point edges in the interband spectrum (see Fig. 9 of the preceding paper). This idea can be tested experimentally by studying the spectra of annealed Xe (Fig. 1), unannealed Xe (Fig. 6) and liquid Xe. In annealed Xe both L excitons are strong. In unannealed Xe the interband scattering structure of the L edges is broadened but is qualitatively unchanged. The $L(\frac{1}{2})$ exciton has apparently "dissolved" into the broad scattering background, and the apparent intensity of the $L(\frac{3}{2})$ exciton is much reduced. Both of these effects can be explained in terms of very strong lifetime broadening, especially for L excitons, by neutral lattice defects in the unannealed films.[28] Note that the configuration interaction of the L excitons with the $\Gamma(\frac{1}{2})$ Rydberg series is also qualitatively unchanged on going from the annealed to the unannealed crystal.

If we now measure the spectrum of liquid Xe, we expect to see the following:

(1) The $\Gamma(\frac{3}{2})$ excitons should be qualitatively similar to those seen in the unannealed film. The $2s$ exciton may still appear as a high-energy shoulder to the $1s$ exciton, and a plateau associated with the series limit may still be resolved.

(2) There should be *no* interband scattering structure above 11.5 eV associated with L or X edges, because the anisotropic Brillouin zone has no meaning in the liquid. In contrast to unannealed Xe, no L exciton resonances at all are expected. This is not a question of lifetime broadening; in the liquid phase no L resonances exist.

(3) Because the L excitons do not exist in the liquid, apart from lifetime effects the $\Gamma(\frac{1}{2})$ excitons should

[28] K. P. Jain (to be published).

[29] A. M. Lane and R. G. Thomas, Rev. Mod. Phys. **30**, 317 (1958), (Fig. 2).

resemble the $\Gamma(\frac{3}{2})$ excitons; in particular, the binding energies should be much more nearly equal than in the solid films. In order to test this point it is necessary that for the $\Gamma(\frac{1}{2})$ excitons either $2s$ or plateau edge (series limit) be resolved in the liquid. From the unannealed spectrum this seems feasible. If the predicted similarity of the $\Gamma(\frac{1}{2})$ series to the $\Gamma(\frac{3}{2})$ series in the liquid is found experimentally, it will provide strong support for our over-all viewpoint.

ACKNOWLEDGMENTS

It is a pleasure to thank G. Baldini for stimulating discussions, and W. B. Fowler for stimulating correspondence.

PHYSICAL REVIEW VOLUME 136, NUMBER 6A 14 DECEMBER 1964

Ultraviolet Absorption of Insulators. V. The Cesium Halides*

J. C. PHILLIPS†
Department of Physics and Institute for the Study of Metals, University of Chicago, Chicago, Illinois
(Received 22 April 1964)

The intrinsic ultraviolet spectra of the simple cubic Cs halides measured by Eby, Teegarden, and Dutton are analyzed into exciton and scattering parts. The effects of configuration interaction on spin-orbit splittings are discussed semiquantitatively, and specific mechanisms are proposed. It is shown that the conduction bands can be separated into a lowest s-like band and higher d-like bands in CsCl and CsBr. In CsI the bands may overlap. The stability of the extra excitons appears to be reduced by configuration interaction in CsI.

1. INTRODUCTION

THIS paper continues the analysis of ultraviolet absorption in insulators previously carried out for tetrahedrally coordinated semiconductors,[1,2] fcc alkali halides,[3] and solid rare gases.[4] Our analysis of the Cs halides is somewhat less complete than previously. The reasons for this are:

(1) The spin-orbit splitting which was so useful for other insulators is less helpful here. In the other insulators the spin-orbit splitting of valence p states followed closely the atomic splittings, while the conduction band splittings were negligible. In the Cs halides, as discussed in Sec. 2, the valence splittings are anomalous.

(2) No complete band calculations are available for the conduction bands of the Cs halides. This difficulty also limited our work on fcc alkali halides, but there we were able to take advantage of band studies[5] of fcc Ar. It turned out that d bands play an important role, which we expect to be even larger in the Cs halides in accordance with the trends of alkali metals. The valence and conduction bands are constructed schematically in Secs. 3 and 4. The uv spectra are analyzed into exciton and scattering parts in Secs. 5 and 6.

2. SPIN-ORBIT SPLITTINGS

In the predominantly covalent group IV and III–V semiconductors the spin-orbit splitting of the valence band at $\mathbf{k}=0$ can be represented as the one-electron average of the splittings on the two atoms in the unit cell. In the III–V compounds the "neutral atom" average

$$\bar{\lambda}=0.35\lambda_{III}+0.65\lambda_V \qquad (2.1)$$

yields good agreement with experiment[6] over a range of λ_{III}/λ_V ratios from 0.03 to 5.4.

In predominantly ionic crystals it has been known for some time that there are systematic deviations from free-atom splittings.[7] These are usually lumped together under the heading of configuration interaction. The early data on substitutional Tl and Pb impurities in the alkali halides have been reviewed by Knox.[8] He mentions a number of possible configuration interactions without specifically favoring any. As an introduction to the subject of spin-orbit splittings in predominantly ionic crystals, we review the data on substitutional Tl splittings in fcc alkali halides and suggest that it can be understood in terms of three specific effects. The data are shown in Table I.

The free ion splitting of Tl^+ is 1.25 eV. In general, the spin-orbit splitting in the crystal tends to be larger than in the free atom or ion because of compression of

* Supported in part by the National Science Foundation, the U. S. Office of Naval Research, and a general grant to the ISM by ARPA.
† Alfred P. Sloan Fellow.
[1] J. C. Phillips, Phys. Rev. **125**, 1931 (1962).
[2] J. C. Phillips, Phys. Rev. **133**, A452 (1964).
[3] J. C. Phillips, Phys. Rev. **136**, A1705 (1964), Paper III, this issue.
[4] J. C. Phillips, Phys. Rev. **136**, A1714 (1964), Paper IV, this issue.
[5] L. F. Mattheiss, Phys. Rev. **133**, A1399 (1964).
[6] M. Cardona, J. Appl. Phys. **32**, 2151S (1961); L. Liu, Phys. Rev. **126**, 1321 (1962).
[7] J. E. Eby, K. J. Teegarden, and D. B. Dutton, Phys. Rev. **116**, 1099 (1959); referred to as ETD.
[8] R. S. Knox, Phys. Rev. **115**, 1095 (1959).